

## Universal topological marker

Wei Chen *Department of Physics, PUC-Rio, 22451-900 Rio de Janeiro, Brazil*

(Received 21 September 2022; revised 15 November 2022; accepted 23 December 2022; published 10 January 2023)

We elaborate that for topological insulators and topological superconductors described by Dirac models in any dimension and symmetry class, the topological order can be mapped to lattice sites by a universal topological marker. Deriving from a recently discovered momentum-space universal topological invariant, we introduce a topological operator that consists of alternating projectors to filled and empty lattice eigenstates and the position operators, multiplied by the Dirac matrices that are omitted in the Hamiltonian. The topological operator projected to lattice sites yields the topological marker, whose form is explicitly constructed for every topologically nontrivial symmetry class from 1D to 3D. The off-diagonal elements of the topological operator yield a nonlocal topological marker, which decays with a correlation length that diverges at topological phase transitions, and represents a Wannier state correlation function. Various prototype examples, including the Su-Schrieffer-Heeger model, Majorana chain, Chern insulators, Bernevig-Hughes-Zhang model, 2D chiral and helical  $p$ -wave superconductors, lattice model of  $^3\text{He}$  B-phase, and 3D time-reversal-symmetric topological insulators, are employed to demonstrate the ubiquity of our formalism.

DOI: [10.1103/PhysRevB.107.045111](https://doi.org/10.1103/PhysRevB.107.045111)

### I. INTRODUCTION

The celebrated topological order in topological insulators (TIs) and superconductors (TSCs) has been recognized as the principle behind various seemingly unrelated phenomena in these materials [1,2]. The topological phases of these materials are characterized by topological invariants that are derived from the Bloch state of the electrons or quasiparticles in momentum space, which have been well understood within the context of symmetry classification that classifies the Dirac Hamiltonians of these materials according to their symmetries and dimensions [3–6]. On the other hand, it has been pointed out that several kinds of topological invariants can be expressed as real-space quantities completely defined from lattice eigenstates, giving rise to the notion of topological markers. The earliest and most widely investigated example is the Chern marker in 2D time-reversal (TR) symmetry-breaking systems, where the corresponding topological invariant is the Chern number calculated from the momentum integration of Berry curvature [7–10]. Through rewriting the Berry curvature into projectors to the valence and conduction bands, which can further be expressed in terms of projectors to the filled and empty states of the lattice Hamiltonian after a momentum integration, the diagonal element of the resulting Chern operator on lattice site  $\mathbf{r}$  yields the correct Chern number [7]. Since the discovery of the Chern marker, various topological markers have been proposed to generalize this concept to other dimensions and symmetry classes [11–23], and even to periodically driven systems [24,25], which have been proved to be a powerful tool to investigate how the real-space inhomogeneity, such as disorder and interfaces, can influence the topological order locally and globally. In addition, several theoretical proposals suggest that some topological markers may be measured by real-space experiments [26,27].

In this paper, we address two important issues that naturally arise along the development of topological marker theories: (1) First, is it possible to formulate a universal topological marker that can be ubiquitously applied to lattice models of TIs and TSCs in any dimension and symmetry class? This question is raised because recently, a wrapping number has been proposed as the universal momentum-space topological invariant in any dimension and symmetry class [28], which has the physical meaning as the number of times that the Brillouin zone (BZ) torus  $T^D$  wraps around the target sphere  $S^D$  of the Dirac Hamiltonian. Similar to the derivation of the Chern marker from rewriting the Chern number into real space [7], we demonstrate that the wrapping number can always be expressed in real space as the trace of an object that we call the topological operator. The diagonal element of the topological operator at lattice site  $\mathbf{r}$  then corresponds in a universal topological marker. (2) Second, can topological phase transitions (TPTs) also be detected in real space by some universal quantity valid for any dimension and symmetry class? This question arises because the integrand of the wrapping number, which plays the role of the Jacobian of the aforementioned  $T^D \rightarrow S^D$  map, has a universal critical behavior in Dirac models; namely, it narrows and flips sign at the gap-closing high-symmetry point  $\mathbf{k}_0$  as the system crosses TPTs [29–33]. We show that this critical behavior can be detected ubiquitously by the  $(\mathbf{r} + \mathbf{R}, \mathbf{r})$ th off-diagonal element of the topological operator that we call the nonlocal topological marker, which is equivalently the Fourier transform of the Jacobian that narrows and flips sign, and thus decays in real space with a decay length that diverges at TPTs.

The structure of the paper is organized in the following manner. In Sec. II, we introduce the formalism that rewrites the wrapping number into projectors to valence and conduction band states, and how it can further be expressed in terms

of filled and empty lattice eigenstates, yielding the topological operator. The local and nonlocal topological markers are further introduced as the diagonal and off-diagonal elements of the topological operator, respectively, and their interpretations in terms of Wannier states are given. In Secs. III–V, we explicitly construct the topological operator for the topologically nontrivial symmetry classes in 3D, 2D, and 1D, and examine various prototype lattice models to demonstrate the universal features of the local and nonlocal topological markers. Section VI summarizes the results, and lists a numbers of open questions that remain to be explored.

## II. GENERAL FORMALISM IN ANY DIMENSION AND SYMMETRY CLASS

### A. Topological operators

Our aim is to formulate a real-space topological marker for TIs and TSCs in  $D$  dimensions described by Dirac Hamiltonian  $H = \mathbf{d}(\mathbf{k}) \cdot \mathbf{\Gamma}$ , where  $\Gamma_i = (\Gamma_0, \Gamma_1, \dots, \Gamma_{2n})$  are the  $n$ th order Dirac matrices of dimension  $2^n \times 2^n$  that satisfy  $\{\Gamma_i, \Gamma_j\} = 2\delta_{ij}$ , and  $\mathbf{d}(\mathbf{k}) = (d_0, d_1, \dots, d_D)$  characterizes the momentum dependence of the Hamiltonian [3,4,6]. It is often more convenient to work on the spectrally flattened Dirac Hamiltonian  $\tilde{Q} = \mathbf{n}(\mathbf{k}) \cdot \mathbf{\Gamma}$  at momentum  $\mathbf{k}$ , where  $\mathbf{n} = \mathbf{d}/|\mathbf{d}|$  is a momentum-dependent unit vector. The precise form of the  $\Gamma$  matrices depends on the dimension and symmetry class of the system at hand. Nevertheless, it has recently been discovered that all the dimensions and symmetry classes can be described by a universal topological invariant calculated from momentum integration of the cyclic derivative of the  $\mathbf{d}$ -vector or  $\mathbf{n}$ -vector,

$$\begin{aligned} \text{deg}[\mathbf{n}] &= \frac{1}{V_D} \int d^D \mathbf{k} \varepsilon_{i_0 \dots i_D} \frac{1}{|\mathbf{d}|^{D+1}} d^{i_0} \partial_1 d^{i_1} \dots \partial_D d^{i_D} \\ &= \frac{1}{V_D} \int d^D \mathbf{k} \varepsilon_{i_0 \dots i_D} n^{i_0} \partial_1 n^{i_1} \dots \partial_D n^{i_D}, \end{aligned} \quad (1)$$

where  $\varepsilon_{i_0 \dots i_D}$  is the fully antisymmetric Levi-Civita symbol. The  $\text{deg}[\mathbf{n}]$  in Eq. (1) has been referred to as the wrapping number or degree of the map that counts the number of times the  $T^D$  BZ wraps around the unit sphere  $S^D$  that the  $\mathbf{n}$ -vector forms, and the integrand  $J_{\mathbf{k}} = \varepsilon_{i_0 \dots i_D} n^{i_0} \partial_1 n^{i_1} \dots \partial_D n^{i_D}$  is the Jacobian of the map [28]. Here  $V_D = 2\pi^{(D+1)/2}/\Gamma(\frac{D+1}{2})$  is the volume of the  $D$ -sphere of unit radius, and  $\partial_j \equiv \partial/\partial k_j$ . The true topological invariant is either  $\text{deg}[\mathbf{n}]$  if the system belongs to the so-called primary or complex series,  $2 \text{deg}[\mathbf{n}]$  for the even series, and  $(-1)^{\text{deg}[\mathbf{n}]}$  for the first and second descendants.

We now elaborate that the  $\text{deg}[\mathbf{n}]$  in Eq. (1) can be expressed as the momentum integration of the trace  $\text{Tr}[W\tilde{Q}(d\tilde{Q})^D]$ , where

$$\tilde{Q}(d\tilde{Q})^D \equiv \tilde{Q} \partial_1 \tilde{Q} \partial_2 \tilde{Q} \dots \partial_D \tilde{Q}, \quad (2)$$

and  $W$  is the product of Dirac matrices that are omitted in the Dirac Hamiltonian for the system at hand, or the identity matrix  $W = I$  if all the Dirac matrices are used. This connection is made because the trace of the product of all the  $n$ th-order  $\Gamma$  matrices is a constant

$$\text{Tr}[\Gamma_0 \Gamma_1 \dots \Gamma_{2n}] = 2^n c, \quad (3)$$

where the prefactor  $c = \{1, -1, i, -i\}$  depends on the representation of the  $\Gamma$  matrices for the system at hand. Now suppose for a specific TI or TSC, the Dirac Hamiltonian uses only  $\{\Gamma_0, \Gamma_1, \dots, \Gamma_D\}$ , leaving  $\{\Gamma_{D+1}, \Gamma_{D+2}, \dots, \Gamma_{2n}\}$  unused. If we define the product of all the unused ones to be  $W = \Gamma_{D+1} \Gamma_{D+2} \dots \Gamma_{2n}$ , it then follows that (repeating indices are summed)

$$\begin{aligned} \text{Tr}[W\tilde{Q}(d\tilde{Q})^D] &= \text{Tr}[\Gamma_{D+1} \Gamma_{D+2} \dots \Gamma_{2n} \Gamma_{i_0} \Gamma_{i_1} \dots \Gamma_{i_D}] n^{i_0} \partial_1 n^{i_1} \dots \partial_D n^{i_D} \\ &= 2^n c \varepsilon_{i_0 \dots i_D} n^{i_0} \partial_1 n^{i_1} \dots \partial_D n^{i_D}, \end{aligned} \quad (4)$$

where the antisymmetric factor  $\varepsilon_{i_0 \dots i_D}$  comes from the fact that the  $\Gamma$  matrices anticommute, and the trace is nonzero and given by Eq. (3) only if every  $\Gamma$  matrix appears once and only once. Taking a momentum integration and comparing with Eq. (1), we obtain

$$\text{deg}[\mathbf{n}] = \frac{(2\pi)^D}{2^n c V_D} \int \frac{d^D \mathbf{k}}{(2\pi)^D} \text{Tr}[W\tilde{Q}(d\tilde{Q})^D]. \quad (5)$$

This quantity  $\int d^D \mathbf{k} \text{Tr}[W\tilde{Q}(d\tilde{Q})^D]$  is our bridge to a real-space topological marker, because it allows us to adopt the projector algebra that originally derives the Chern marker [7]. To see this, we observe that the spectrally flattened Hamiltonian  $\tilde{Q}$  can be separated into the projector  $p$  into the valence band states  $|n(\mathbf{k})\rangle$  and the projector  $q$  into the conduction band states  $|m(\mathbf{k})\rangle$ ,

$$\tilde{Q} = q - p, \quad p = \sum_n |n\rangle\langle n|, \quad q = \sum_m |m\rangle\langle m|, \quad (6)$$

and  $q + p = I$ . As a result, the derivative of  $\tilde{Q}$  over a certain component of momentum  $\partial/\partial k_j \equiv \partial_j$  is equivalently  $\partial_i \tilde{Q} = 2\partial_i q = -2\partial_i p$ . Consequently, we can write  $\tilde{Q}(d\tilde{Q})^D$  into the form that consists of alternating derivatives of  $p$  and  $q$ .

Consider first  $D = \text{odd}$ , in which case the integrand of Eq. (5) can be written as

$$\begin{aligned} W\tilde{Q}(d\tilde{Q})^D|_{D=\text{odd}} &= 2^D (-1)^{(D+1)/2} W \{q \partial_1 p \partial_2 q \dots \partial_D p + p \partial_1 q \partial_2 p \dots \partial_D q\} \\ &= 2^D (-1)^{(D+1)/2} \sum_{m_1 \sim m_{(D+1)/2}} \sum_{n_1 \sim n_{(D+1)/2}} W \{ |m_1\rangle\langle m_1| \partial_{i_1} n_1 \langle n_1| \partial_{i_2} m_2 \rangle \dots \\ &\quad \dots \langle m_{(D+1)/2} | \partial_{i_D} n_{(D+1)/2} \rangle \langle n_{(D+1)/2} | + (m \leftrightarrow n) \}, \end{aligned} \quad (7)$$

where  $|\partial n_i\rangle\langle n_i|$  comes from the  $i$ th  $p$  operator on the second line of this equation,  $|\partial m_i\rangle\langle m_i|$  comes from the  $i$ th  $q$  operator, and each operator appears  $(D+1)/2$  times. The motivation to rewrite it into this form of alternating  $p$  and  $q$  is to use the identity [7]

$$\langle m | \partial_i | n \rangle = -i \langle \psi_m | \hat{i} | \psi_n \rangle, \quad (8)$$

provided  $n \neq m$ , where the  $|\psi_n\rangle = |\psi_n(\mathbf{k})\rangle$  is the full wave function that satisfies  $\langle \mathbf{r} | \psi_n(\mathbf{k}) \rangle = \psi_{n\mathbf{k}}(\mathbf{r}) = u_{n\mathbf{k}}(\mathbf{r}) e^{i\mathbf{k}\cdot\mathbf{r}} = \langle \mathbf{r} | n(\mathbf{k}) \rangle e^{i\mathbf{k}\cdot\mathbf{r}}$  with  $u_{n\mathbf{k}}(\mathbf{r})$  the Bloch periodic part of the wave function. Here  $\hat{i}$  is the position operator, which is a diagonal matrix where all the  $2^n$  internal degrees of freedom (spin, orbit, particle-hole, etc.) within a unit cell located at the Bravais lattice vector  $\mathbf{r} = (x, y, z, \dots)$  are assigned with the same  $\mathbf{r}$ . This identity allows us to write

$$\begin{aligned} & \int \frac{d^D \mathbf{k}}{(2\pi)^D} \text{Tr}[W \tilde{Q} (d\tilde{Q})^D]_{D \in \text{odd}} \\ &= 2^D i \int \frac{d^D \mathbf{k}}{(2\pi)^D} \varepsilon^{i_1 i_2 \dots i_D} \sum_{m_1 \sim m_{(D+1)/2}} \sum_{n_1 \sim n_{(D+1)/2}} \text{Tr}\{W |\psi_{m_1}\rangle \langle \psi_{m_1}| \hat{i}_1 |\psi_{n_1}\rangle \langle \psi_{n_1}| \dots \langle \psi_{m_{(D+1)/2}} | \hat{i}_D | \psi_{n_{(D+1)/2}} \rangle \langle \psi_{n_{(D+1)/2}} | + (m \leftrightarrow n)\} \\ &= 2^D i \text{Tr} \left[ W \int \frac{d^D \mathbf{k}_{m_1}}{(2\pi)^D} \sum_{m_1} |\psi_{m_1}\rangle \langle \psi_{m_1}| \hat{i}_1 \int \frac{d^D \mathbf{k}_{n_1}}{(2\pi)^D} \sum_{n_1} |\psi_{n_1}\rangle \langle \psi_{n_1}| \hat{i}_2 \dots \int \frac{d^D \mathbf{k}_{m_{(D+1)/2}}}{(2\pi)^D} \sum_{m_{(D+1)/2}} |\psi_{m_{(D+1)/2}}\rangle \langle \psi_{m_{(D+1)/2}}| \hat{i}_D \right. \\ & \quad \left. \times \int \frac{d^D \mathbf{k}_{n_{(D+1)/2}}}{(2\pi)^D} \sum_{n_{(D+1)/2}} |\psi_{n_{(D+1)/2}}\rangle \langle \psi_{n_{(D+1)/2}}| + (n \leftrightarrow m) \right]. \end{aligned} \quad (9)$$

In the last step, we identify the projector to the valence bands integrated over momentum as the projector to the filled band states  $|E_n\rangle$  of a lattice Hamiltonian, and likewise the projector to the conduction bands integrated over momentum as the projector to the empty band states  $|E_m\rangle$

$$\int \frac{d^D \mathbf{k}_{m_j}}{(2\pi)^D} \sum_{m_j} |\psi_{m_j}\rangle \langle \psi_{m_j}| = \sum_m |E_m\rangle \langle E_m| \equiv Q, \quad \int \frac{d^D \mathbf{k}_{n_j}}{(2\pi)^D} \sum_{n_j} |\psi_{n_j}\rangle \langle \psi_{n_j}| = \sum_n |E_n\rangle \langle E_n| \equiv P, \quad (10)$$

which are  $(L^D 2^n) \times (L^D 2^n)$  matrices, where  $L^D$  is the total number of unit cells in the lattice, and each unit cell contains  $2^n$  degrees of freedom. Equation (9) then becomes

$$\int \frac{d^D \mathbf{k}}{(2\pi)^D} \text{Tr}[W \tilde{Q} (d\tilde{Q})^D]_{D \in \text{odd}} = 2^D i \text{Tr}[W Q \hat{i}_1 P \hat{i}_2 \dots Q \hat{i}_D P + W P \hat{i}_1 Q \hat{i}_2 \dots P \hat{i}_D Q], \quad (11)$$

where in the second line we have enlarged  $W \rightarrow W \otimes I_{L^D \times L^D}$ . Note that in Eq. (11), the trace on the left-hand side is over the  $2^n$  internal degrees of freedom at momentum  $\mathbf{k}$ , whereas the trace on the right-hand side is over the  $2^n \times L^D$  degrees of freedom on a lattice Hamiltonian of  $L^D$  unit cells. In this way we have written the momentum-space topological invariant into an object that is completely defined from the eigenstates of a lattice Hamiltonian.

In  $D = \text{even}$  dimensions, the construction is similar. We again seek to write the integrand  $W \tilde{Q} (d\tilde{Q})^D$  into alternating derivatives of  $p$  and  $q$ , which in even dimensions becomes

$$\begin{aligned} W \tilde{Q} (d\tilde{Q})^D |_{D \in \text{even}} &= 2^D (-1)^{D/2} W \{q \partial_{i_1} p \partial_{i_2} q \dots \partial_{i_D} q - p \partial_{i_1} q \partial_{i_2} p \dots \partial_{i_D} p\} \\ &= 2^D (-1)^{D/2} \sum_{m_1 \sim m_{D/2+1}} \sum_{n_1 \sim n_{D/2}} W \{|m_1\rangle \langle m_1| \partial_{i_1} n_1 \langle n_1| \partial_{i_2} m_2 \rangle \dots \langle n_{D/2} | \partial_{i_D} m_{D/2+1} \rangle \langle m_{D/2+1} | - (m \leftrightarrow n)\}, \end{aligned} \quad (12)$$

where  $p$  appears  $D/2$  times and  $q$  appears  $D/2 + 1$  times for the first array in the second line of this equation, and vice versa for the second array. The momentum integration of this quantity becomes

$$\begin{aligned} & \int \frac{d^D \mathbf{k}}{(2\pi)^D} \text{Tr}[W \tilde{Q} (d\tilde{Q})^D]_{D \in \text{even}} \\ &= 2^D \int \frac{d^D \mathbf{k}}{(2\pi)^D} \sum_{m_1 \sim m_{D/2+1}} \sum_{n_1 \sim n_{D/2}} \text{Tr}\{W |\psi_{m_1}\rangle \langle \psi_{m_1}| \hat{i}_1 |\psi_{n_1}\rangle \langle \psi_{n_1}| \dots \langle \psi_{n_{D/2}} | \hat{i}_D | \psi_{m_{D/2+1}} \rangle \langle \psi_{m_{D/2+1}} | - (m \leftrightarrow n)\} \\ &= 2^D \text{Tr} \left[ W \int \frac{d^D \mathbf{k}_{m_1}}{(2\pi)^D} \sum_{m_1} |\psi_{m_1}\rangle \langle \psi_{m_1}| \hat{i}_1 \int \frac{d^D \mathbf{k}_{n_1}}{(2\pi)^D} \sum_{n_1} |\psi_{n_1}\rangle \langle \psi_{n_1}| \hat{i}_2 \dots \int \frac{d^D \mathbf{k}_{n_{D/2}}}{(2\pi)^D} \sum_{n_{D/2}} |\psi_{n_{D/2}}\rangle \langle \psi_{n_{D/2}}| \hat{i}_D \right. \\ & \quad \left. \times \int \frac{d^D \mathbf{k}_{m_{D/2+1}}}{(2\pi)^D} \sum_{m_{D/2+1}} |\psi_{m_{D/2+1}}\rangle \langle \psi_{m_{D/2+1}}| - (n \leftrightarrow m) \right]. \end{aligned} \quad (13)$$

Using the projectors in Eq. (10), we arrive at

$$\int \frac{d^D \mathbf{k}}{(2\pi)^D} \text{Tr}[W \tilde{Q} (d\tilde{Q})^D]_{D \in \text{even}} = 2^D \text{Tr}[W Q \hat{i}_1 P \hat{i}_2 \dots P \hat{i}_D Q - W P \hat{i}_1 Q \hat{i}_2 \dots Q \hat{i}_D P]. \quad (14)$$

Once again we have written the topological invariant into a form that is completely defined from the lattice eigenstates.

Equations (11) and (14) suggest a universal topological operator of the form

$$\hat{C} = N_D W [Q \hat{i}_1 P \hat{i}_2 \dots \hat{i}_D \mathcal{O} + (-1)^{D+1} P \hat{i}_1 Q \hat{i}_2 \dots \hat{i}_D \bar{\mathcal{O}}], \quad (15)$$

where the last operators  $\{\mathcal{O}, \bar{\mathcal{O}}\} = \{P, Q\}$  if  $D = \text{odd}$ , and  $\{\mathcal{O}, \bar{\mathcal{O}}\} = \{Q, P\}$  if  $D = \text{even}$  owing to the alternating ordering of the projectors  $Q$  and  $P$ . Using Eqs. (5), (11), and (14), one sees that the wrapping number in Eq. (1) is equal to the trace of this operator,

$$\text{deg}[\mathbf{n}] = \frac{1}{L^D} \text{Tr}[\hat{C}], \quad (16)$$

where  $L^D$  is the total number of unit cells, and  $\text{Tr}[\dots]$  represents the trace over all the lattice sites. The normalization factor  $N_D$  in Eq. (15) has the expression

$$N_D = \frac{i^D 2^{2D-n} \pi^D}{c V_D}, \quad (17)$$

which depends on the dimension  $D$ , the volume  $V_D = \{V_1, V_2, V_3, \dots\} = \{2\pi, 4\pi, 2\pi^2, \dots\}$ , the order  $n$ , and the prefactor  $c = \text{Tr}[\Gamma_0 \Gamma_1 \dots \Gamma_{2n}] / 2^n = \{1, -1, i, -i\}$  of the representation of  $\Gamma$  matrices for the system under question. Equations (15) to (17) are the central results of this work, and we will demonstrate their validity using concrete models in the following sections.

### B. Local and nonlocal topological markers

Similar to the original construction of Chern marker as the diagonal elements of Chern operator [7], the correspondence between the wrapping number and the trace of the topological operator in Eq. (16) suggests defining the (local) topological marker on a lattice site  $\mathbf{r}$  by

$$\mathcal{C}(\mathbf{r}) = \langle \mathbf{r} | \hat{C} | \mathbf{r} \rangle = \sum_{\sigma} \langle \mathbf{r} \sigma | \hat{C} | \mathbf{r} \sigma \rangle; \quad (18)$$

i.e., the marker is the diagonal element of topological operator at  $\mathbf{r}$ . Here  $\sum_{\sigma}$  represents the summation over all the  $2^n$  internal degrees of freedom inside the unit cell at  $\mathbf{r}$ , such as spin, orbital, and particle-hole.

We further introduce a nonlocal topological marker as the  $(\mathbf{r} + \mathbf{R}, \mathbf{r})$ th off-diagonal matrix element of the topological operator [26,27]

$$\mathcal{C}(\mathbf{r} + \mathbf{R}, \mathbf{r}) = \langle \mathbf{r} + \mathbf{R} | \hat{C} | \mathbf{r} \rangle, \quad (19)$$

where  $\mathbf{R}$  is a Bravais lattice vector. For a homogeneous lattice model in the thermodynamic limit, this nonlocal marker is independent of  $\mathbf{r}$ , and is equivalently the Fourier transform of the integrand of the wrapping number in Eq. (1),

$$\begin{aligned} \mathcal{C}(\mathbf{r} + \mathbf{R}, \mathbf{r}) &= \tilde{F}(\mathbf{R}) \\ &\equiv \frac{1}{V_D} \int d^D \mathbf{k} \varepsilon_{i_0 \dots i_D} n^{i_0} \partial_1 n^{i_1} \dots \partial_D n^{i_D} e^{i \mathbf{k} \cdot \mathbf{R}}, \end{aligned} \quad (20)$$

that has been previously denoted by  $\tilde{F}(\mathbf{R})$  [31–33], and has the physical meaning as a correlation function that measures the overlap between Wannier states that are a distance  $\mathbf{R}$  apart,

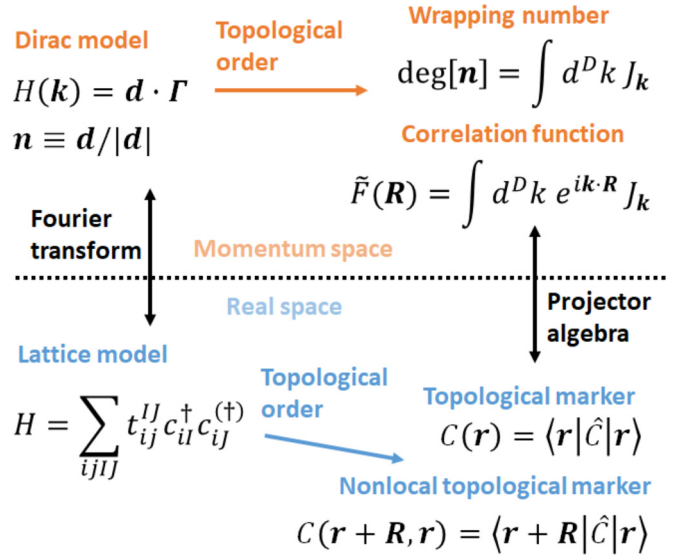


FIG. 1. Summary of the correspondence between the topological order in momentum space calculated from the Jacobian  $J_{\mathbf{k}} = \varepsilon_{i_0 \dots i_D} n^{i_0} \partial_1 n^{i_1} \dots \partial_D n^{i_D}$ , where  $n^i$  characterizes the spectrally flattened Dirac Hamiltonian  $\hat{Q} = \mathbf{n} \cdot \Gamma$ , and that in real space calculated from the topological operator  $\mathcal{C}$  constructed from projectors and position operators. For homogeneous systems in the thermodynamic limit, the wrapping number is equal to the topological marker  $\text{deg}[\mathbf{n}] = \mathcal{C}(\mathbf{r})$ , and the Wannier state correlation function is equivalently the nonlocal topological marker  $\tilde{F}(\mathbf{R}) = \mathcal{C}(\mathbf{r} + \mathbf{R}, \mathbf{r})$ .

as we shall see in Sec. II C. The identification  $\mathcal{C}(\mathbf{r} + \mathbf{R}, \mathbf{r}) = \tilde{F}(\mathbf{R})$  can be seen by considering equivalently the Fourier transform of  $\text{Tr}[W \hat{Q}(d \hat{Q})^D]$ , which contains the projection  $\langle \mathbf{r} | W | \psi_{m_1} \rangle e^{i \mathbf{k} \cdot \mathbf{R}}$  of the first ket state of Eqs. (9) and (13) that is equal to  $\langle \mathbf{r} + \mathbf{R} | W | \psi_{m_1} \rangle$ ,

$$\begin{aligned} \langle \mathbf{r} | W | \psi_{m_1} \rangle e^{i \mathbf{k} \cdot \mathbf{R}} &= e^{i \mathbf{k}(\mathbf{r} + \mathbf{R})} W u_{m_1 \mathbf{k}}(\mathbf{r} + \mathbf{R}) \\ &= W \psi_{m_1 \mathbf{k}}(\mathbf{r} + \mathbf{R}) = \langle \mathbf{r} + \mathbf{R} | W | \psi_{m_1} \rangle, \end{aligned} \quad (21)$$

owing to the cell periodicity of the Bloch state  $u_{m_1 \mathbf{k}}(\mathbf{r} + \mathbf{R}) = u_{m_1 \mathbf{k}}(\mathbf{r})$ . The correspondence between the momentum-space topological invariants and the real-space topological markers is summarized schematically in Fig. 1.

The spatial profile of the nonlocal marker  $\mathcal{C}(\mathbf{r} + \mathbf{R}, \mathbf{r})$  decays with  $\mathbf{R}$ , with a decay length  $\xi$  that diverges at TPTs, thereby serving as a faithful quantity to identify TPTs. This can be seen by considering the linear Dirac model  $d^0 = M$ ,  $d^{i \neq 0} = v k_i$ , which is a low-energy effective model near the gap-closing momentum that describes the majority of TPTs. The integrand of Eq. (1) has a Lorentzian shape in this model,

$$\begin{aligned} \varepsilon_{i_0 \dots i_D} \frac{1}{|\mathbf{d}|^{D+1}} d^{i_0} \partial_1 d^{i_1} \dots \partial_D d^{i_D} &= \frac{M}{[M^2 + v^2 k^2]^{(D+1)/2}} \\ &\approx \frac{\text{sgn}(M) |M|^{-D}}{1 + \xi^2 k^2}, \end{aligned} \quad (22)$$

implying that its Fourier transform  $\mathcal{C}(\mathbf{r} + \mathbf{R}, \mathbf{r})$  decays with a correlation length  $\xi \sim |M|^{-\nu}$  that diverges at the critical point  $M_c = 0$ , with the critical exponent  $\nu = 1$ . In addition, owing to the relation between the integrand and the quantum metric of the valence band state [34], a relation that has been called

the metric-curvature correspondence [35], the integrand at  $\mathbf{k} = 0$  that scales like  $\sim |M|^{-D}$  has the meaning as the fidelity susceptibility near TPTs [36], and hence has been assigned with the exponent  $\gamma = D$ .

Generally, a  $D$ -dimensional cubic lattice model contains multiple critical points  $M_c$ , each corresponding to gap closing at a specific high-symmetry point (HSP)  $\mathbf{k}_0 = (k_{0x}, k_{0y}, \dots)$ , where  $k_{0j} = 0$  or  $\pi$ . The integrand of Eq. (1) also peaks at the corresponding HSP; i.e., the  $\mathbf{k}$  in Eq. (22) is actually the momentum away from the HSP. As a result, if the HSP is not at the  $\Gamma$  point of the BZ, then the nonlocal topological marker will oscillate in real space besides decaying, since in this case

$$\begin{aligned} \mathcal{C}(\mathbf{r} + \mathbf{R}, \mathbf{r}) & \approx \frac{1}{V_D} \int d^D \mathbf{k} \frac{\text{sgn}(M - M_c) |M - M_c|^{-D}}{1 + \xi^2 k^2} e^{i(\mathbf{k} - \mathbf{k}_0) \cdot \mathbf{R}} \\ & = e^{-i\mathbf{k}_0 \cdot \mathbf{R}} \mathcal{F}(\mathbf{R}), \end{aligned} \quad (23)$$

where  $\mathcal{F}(\mathbf{R})$  decays with  $\mathbf{R}$  as argued above. One sees that the nonlocal marker also oscillates in the  $j$ th direction where

$$\begin{aligned} \mathcal{C}(\mathbf{r})|_{D \in \text{odd}} & \propto \int \frac{d^D \mathbf{k}}{(2\pi)^D} \text{Tr}[W \tilde{Q}(d\tilde{Q})^D]_{D \in \text{odd}} = 2^D i \varepsilon^{i_1 \dots i_D} \sum_{\mathbf{R}_1 \sim \mathbf{R}_{2D+1}} \sum_{m_1 \sim m_{(D+1)/2}} \sum_{n_1 \sim n_{(D+1)/2}} \langle \mathbf{R}_1 n_{(D+1)/2} | W | \mathbf{R}_2 m_1 \rangle \langle \mathbf{R}_3 m_1 | \hat{i}_1 | \mathbf{R}_4 n_1 \rangle \dots \\ & \quad \langle \mathbf{R}_{2D+1} m_{(D+1)/2} | \hat{i}_D | (\mathbf{R}_1 - \mathbf{R}_2 + \dots + \mathbf{R}_{2D+1}) n_{(D+1)/2} \rangle + (n \leftrightarrow m), \end{aligned} \quad (25)$$

and a similar one in  $D = \text{even}$  dimensions

$$\begin{aligned} \mathcal{C}(\mathbf{r})|_{D \in \text{even}} & \propto \int \frac{d^D \mathbf{k}}{(2\pi)^D} \text{Tr}[W \tilde{Q}(d\tilde{Q})^D]_{D \in \text{even}} = 2^D \varepsilon^{i_1 \dots i_D} \sum_{\mathbf{R}_1 \sim \mathbf{R}_{2D+1}} \sum_{m_1 \sim m_{D/2+1}} \sum_{n_1 \sim n_{D/2}} \langle \mathbf{R}_1 m_{D/2+1} | W | \mathbf{R}_2 m_1 \rangle \langle \mathbf{R}_3 m_1 | \hat{i}_1 | \mathbf{R}_4 n_1 \rangle \dots \\ & \quad \langle \mathbf{R}_{2D+1} n_{D/2} | \hat{i}_D | (\mathbf{R}_1 - \mathbf{R}_2 + \mathbf{R}_3 \dots + \mathbf{R}_{2D+1}) m_{D/2+1} \rangle - (n \leftrightarrow m). \end{aligned} \quad (26)$$

Likewise, the nonlocal topological markers  $\mathcal{C}(\mathbf{r} + \mathbf{R}, \mathbf{r})$  in the homogeneous limit in either even or odd dimensions can also be expressed in terms of Wannier states, which is simply given by the results in Eq. (26) with the last position argument replaced by  $(\mathbf{R}_1 - \mathbf{R}_2 + \mathbf{R}_3 \dots + \mathbf{R}_{2D+1}) \rightarrow (\mathbf{R}_1 - \mathbf{R}_2 + \mathbf{R}_3 \dots + \mathbf{R}_{2D+1} - \mathbf{R})$ . As a result, the nonlocal marker  $\mathcal{C}(\mathbf{r} + \mathbf{R}, \mathbf{r})$  has the physical meaning as the measure of the overlap of Wannier states weighted by the position operators, which decays with  $\mathbf{R}$  according to the argument after Eq. (22). Moreover, the decay length  $\xi$  diverges at TPTs, and hence  $\mathcal{C}(\mathbf{r} + \mathbf{R}, \mathbf{r})$  serves as a faithful correlator that characterizes the quantum criticality near TPTs. Finally, we also mention that although this Wannier state formalism nicely interprets the nonlocal marker as a correlator, one need not calculate the correlator directly from the Wannier states, which may be quite tedious. Instead, one can easily extract it from the off-diagonal elements of the topological operator as described by Eq. (19), as we shall see in the following sections.

#### D. Applications to lattice models from 1D to 3D

The TIs and TSCs can be classified according to the TR, particle-hole (PH), and chiral symmetries of the system, with the corresponding symmetry operators denoted by  $T$ ,  $C$ , and  $S$ , respectively. These symmetries are said to be satisfied if the

$k_{0j} = \pi$  owing to the  $e^{-i\mathbf{k}_0 \cdot \mathbf{R}}$  factor. For instance, if in a 3D cubic lattice model the gap closes at  $\mathbf{k}_0 = (k_{0x}, k_{0y}, k_{0z}) = (\pi, \pi, 0)$ , then the nonlocal marker will oscillate in both the  $\hat{x}$  and  $\hat{y}$  directions, but not in the  $\hat{z}$  direction. We shall see some concrete examples in the following sections.

#### C. Wannier state representations

We proceed to elaborate that in the homogeneous and thermodynamic limit, both the local and nonlocal topological markers can be expressed in terms of overlap of Wannier states. Given the Bloch states  $|\ell\rangle = |\ell_{\mathbf{k}}\rangle$  of either the valence  $\ell = n$  or conduction  $\ell = m$  band states, we can introduce the Wannier state  $|\mathbf{R}\ell\rangle$  by

$$|\ell_{\mathbf{k}}\rangle = \sum_{\mathbf{R}} e^{-i\mathbf{k} \cdot (\hat{\mathbf{r}} - \mathbf{R})} |\mathbf{R}\ell\rangle, \quad |\mathbf{R}\ell\rangle = \sum_{\mathbf{k}} e^{i\mathbf{k} \cdot (\hat{\mathbf{r}} - \mathbf{R})} |\ell_{\mathbf{k}}\rangle. \quad (24)$$

Inserting these definitions into Eqs. (9) and (13) yields an expression for the local topological marker in  $D = \text{odd}$  dimensions

single-particle Hamiltonian satisfies [3–6]

$$\begin{aligned} TH(\mathbf{k})T^{-1} & = H(-\mathbf{k}), \quad CH(\mathbf{k})C^{-1} = -H(-\mathbf{k}), \\ SH(\mathbf{k})S^{-1} & = -H(\mathbf{k}), \end{aligned} \quad (27)$$

yielding a total of 10 symmetry classes. The result of the classification gives 5 topologically nontrivial symmetry classes in each spatial dimension  $D$ . For practical reasons, in the following sections, we explicitly construct the topological operators in Eq. (15) for all the 15 nontrivial symmetry classes from 1D to 3D. Moreover, for those classes described by  $2 \times 2$  and  $4 \times 4$  Dirac matrices, which cover 13 out of the 15 nontrivial classes, we will use cubic lattice models to explicitly demonstrate the validity of the local and nonlocal topological markers. The two cases left unexamined are classes CI and CII in 3D described by  $8 \times 8$  Dirac matrices, which are less explored in the literature and will be left for future investigations.

To elaborate the ubiquity of the topological operators and markers, in each lattice model, we choose the periodic boundary condition in all spatial directions, focus on one specific critical point of the mass term  $M_c$ , and examine four parameters of  $M$  denoted by

$$\begin{aligned} M_1 & : \text{nontrivial phase far from } M_c \text{ (red),} \\ M_2 & : \text{nontrivial phase close to } M_c \text{ (green),} \end{aligned}$$

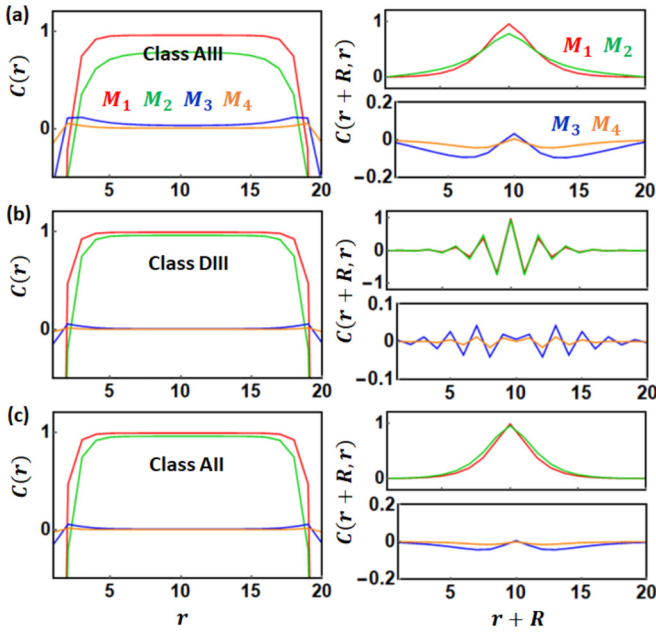


FIG. 2. Local (left column) and nonlocal (right column) topological markers for lattice models in three out of the five topologically nontrivial symmetry classes in 3D, including (a) a regularized lattice model for class AIII, (b) a lattice model of  $^3\text{He}$  B-phase in class DIII, and (c) the prototype 3D TR-symmetric TIs in class AII.

$$\begin{aligned} M_3 : & \text{trivial phase close to } M_c \text{ (blue),} \\ M_4 : & \text{trivial phase far from } M_c \text{ (orange).} \end{aligned} \quad (28)$$

The purpose of examining these 4 parameters is to elaborate that the behavior of local and nonlocal topological markers is the same in any dimension and symmetry class [see the figures in the following sections, with the same color code indicated in Eq. (28)]: Deep inside the bulk,  $M_1$  and  $M_2$  have the same integer-valued topological marker  $\mathcal{C}(\mathbf{r})$  since they are in the same topological phase, but the nonlocal topological marker  $\mathcal{C}(\mathbf{r} + \mathbf{R}, \mathbf{r})$  of  $M_2$  has a longer decay length than  $M_1$  since it is closer to the critical point according to the discussion after Eq. (22). Likewise,  $M_3$  and  $M_4$  have the same  $\mathcal{C}(\mathbf{r})$  deep inside the bulk, but  $M_3$  has a longer decay length of  $\mathcal{C}(\mathbf{r} + \mathbf{R}, \mathbf{r})$  than  $M_4$  since it is closer to the critical point. We also remark that numerically, we find that the local marker at the boundary sites deviates from the bulk value even if the periodic boundary condition is employed. This is a feature well known for this type of construction [7], since the position operators  $\hat{i}$  in Eq. (15) do not respect translational invariance. Such an anomaly may be fixed by exponentiating the position operator [8,10], which shall be explored elsewhere.

### III. TOPOLOGICAL MARKERS IN THREE DIMENSIONS

In 3D TIs and TSCs, the topological operator has the following general form,

$$\hat{\mathcal{C}}_{3D} = N_D W [Q\hat{x}P\hat{y}Q\hat{z}P + P\hat{x}Q\hat{y}P\hat{z}Q]. \quad (29)$$

The  $W$  matrix has different interpretations in different classes. The numerical results for classes AIII, DIII, and AII are presented in Fig. 2 using prototype cubic lattice models simulated

on a 3D lattice of dimension  $L_x \times L_y \times L_z = 20 \times 8 \times 8$ . We use a lattice that is elongated in the  $\hat{x}$  direction and plot the results along this direction for the sake of increasing numerical accuracy. The details of each symmetry class are described below.

#### A. 3D class AIII

In 3D classes AIII, the  $\Gamma$  matrices are given by [4]

$$\begin{aligned} \Gamma_{1\sim 5} &= (\alpha_x, \alpha_y, \alpha_z, \beta, -i\beta\gamma^5), \\ \alpha_i &= \begin{pmatrix} 0 & \sigma_i \\ \sigma_i & 0 \end{pmatrix}, \quad \beta = \begin{pmatrix} 1 & 0 \\ 0 & -1 \end{pmatrix}, \quad \gamma^5 = \begin{pmatrix} 0 & 1 \\ 1 & 0 \end{pmatrix}. \end{aligned} \quad (30)$$

The chiral operator  $S = \beta$  demands  $d^4(\mathbf{k}) = 0$ , so for a linear Dirac model one chooses  $d_1 = Ak_x$ ,  $d_2 = Ak_y$ ,  $d_3 = Ak_z$ , and  $d_5 = M + B \sum_{\ell=1}^3 k_\ell^2$  as the mass term that contains a quadratic term to avoid fermion doubling. The spinor of 3D class AIII contains only annihilation operators, which we name generically as  $\psi = (c_{k1}, c_{k2}, c_{k3}, c_{k4})$ , where  $c_{kJ}$  is the  $J$ th degree of freedom. Regularizing the linear Dirac model in the whole BZ by

$$A k_\ell \rightarrow A \sin k_\ell,$$

$$M \rightarrow M + B \sum_{\ell=1}^D k_\ell^2 \rightarrow M + 2DB - 2B \sum_{\ell=1}^D \cos k_\ell, \quad (31)$$

with  $D = 3$  in this case, we may further construct a cubic lattice Hamiltonian by performing a Fourier transform

$$\begin{aligned} \sum_k \cos k_\ell c_{\mathbf{k}l}^\dagger c_{\mathbf{k}J} &\rightarrow \frac{1}{2} \sum_i \{c_{i\ell}^\dagger c_{i+e_\ell J} + c_{i+e_\ell \ell}^\dagger c_{iJ}\}, \\ \sum_k i \sin k_\ell c_{\mathbf{k}l}^\dagger c_{\mathbf{k}J} &\rightarrow \frac{1}{2} \sum_i \{c_{i\ell}^\dagger c_{i+e_\ell J} - c_{i+e_\ell \ell}^\dagger c_{iJ}\}. \end{aligned} \quad (32)$$

Denoting  $t = A/2$  and  $t' = B$ , the resulting lattice model is

$$\begin{aligned} H &= \sum_i t \{-ic_{i1}^\dagger c_{i+x4} + ic_{i+x1}^\dagger c_{i4} - ic_{i2}^\dagger c_{i+x3} + ic_{i+x2}^\dagger c_{i3}\} \\ &+ \sum_i t \{-c_{i1}^\dagger c_{i+y4} + c_{i+y1}^\dagger c_{i4} + c_{i2}^\dagger c_{i+y3} - c_{i+y2}^\dagger c_{i3}\} \\ &+ \sum_i t \{-ic_{i1}^\dagger c_{i+z3} + ic_{i+z1}^\dagger c_{i3} + ic_{i2}^\dagger c_{i+z4} - ic_{i+z2}^\dagger c_{i4}\} \\ &+ \sum_{i\delta} it' \{c_{i1}^\dagger c_{i+\delta 3} + c_{i+\delta 1}^\dagger c_{i3} + c_{i2}^\dagger c_{i+\delta 4} + c_{i+\delta 2}^\dagger c_{i4}\} \\ &+ \sum_i (-iM - i6t') \{c_{i1}^\dagger c_{i3} + c_{i2}^\dagger c_{i4}\} + \text{H.c.} \end{aligned} \quad (33)$$

The omitted Dirac matrix is the chiral operator  $W = \beta = \Gamma_4 = S$ , and the normalization factor is  $N_D = -8\pi i$ .

The parameters  $t = t' = 0.5$  and  $\{M_1, M_2, M_3, M_4\} = \{-0.5, -0.2, 0.2, 0.5\}$  are used in the numerical simulation. The results shown in Fig. 2(a) clearly demonstrate the features outlined after Eq. (28): Deep inside the bulk, the left panel of Fig. 2(a) indicates that  $M_1$  and  $M_2$  have the same topological marker  $\mathcal{C}(\mathbf{r}) \approx 1$  (red and green lines coincide) because they belong to the same topologically nontrivial phase, and  $M_3$  and  $M_4$  have the same  $\mathcal{C}(\mathbf{r}) \approx 0$  (blue and orange lines coincide)

because they are both topologically trivial. On the other hand, the right panel of Fig. 2(a) shows that the nonlocal marker  $\mathcal{C}(\mathbf{r} + \mathbf{R}, \mathbf{r})$  of  $M_2$  is more long ranged than  $M_1$  (green line extends longer than red line) because  $M_2$  is closer to the critical point  $M_c = 0$ , and  $M_3$  is more long ranged than  $M_4$  (blue line extends longer than orange line) for the same reason. These features are found to be true for all models we have examined in any dimension and symmetry class, as can be clearly identified from Figs. 2–4, with the same color codes that designate  $\{M_1, M_2, M_3, M_4\}$ .

### B. 3D class DIII

A concrete example of 3D class DIII is the B phase of superfluid  $^3\text{He}$  [37,38]. For the purpose of discussing the 2D class DIII case after a dimensional reduction, which will be addressed in Sec. IV E, we use the representation of  $\Gamma$  matrices in the Bernevig-Hughes-Zhang (BHZ) model [39,40]

$$\Gamma^{1\sim 5} = \{s_x \otimes \sigma_z, s_y \otimes I, s_z \otimes I, s_x \otimes \sigma_x, s_x \otimes \sigma_y\}. \quad (34)$$

The TR, PH, and chiral operators in this basis are  $T = -iI \otimes \sigma_y K$ ,  $C = s_x \otimes IK$ , and  $S = \Gamma^5$ . Since we aim to demonstrate the topological marker on a lattice, we regularize the pairing terms of the B phase of  $^3\text{He}$  on a square lattice by  $\Delta k_i \rightarrow \Delta \sin k_i$ , and likewise the kinetic terms, and arrange our spinor according to Eq. (34) by  $\eta_{\mathbf{k}}^\dagger = (c_{\mathbf{k}\uparrow}^\dagger, c_{-\mathbf{k}\uparrow}^\dagger, c_{\mathbf{k}\downarrow}^\dagger, c_{-\mathbf{k}\downarrow}^\dagger)$ . The leads to the parametrization of the Hamiltonian

$$H = \sum_{\mathbf{k}} \eta_{\mathbf{k}}^\dagger \left( \sum_{i=1}^4 d_i \Gamma^i \right) \eta_{\mathbf{k}}, \quad d_1 = \Delta \sin k_x, \quad d_2 = \Delta \sin k_y, \\ d_3 = 2t(\cos k_x + \cos k_y + \cos k_z) - \mu, \quad d_4 = -\Delta \sin k_z, \quad (35)$$

so the unused Dirac matrix is the chiral operator  $W = S = \Gamma^5$ , and the normalization factor is  $N_D = -8\pi i$ . We then construct a square lattice model in a similar manner as Eq. (32), yielding

$$H = \sum_{i\sigma\delta} -t(c_{i\sigma}^\dagger c_{i+\delta\sigma} + c_{i+\delta\sigma}^\dagger c_{i\sigma}) - \mu \sum_{i\sigma} c_{i\sigma}^\dagger c_{i\sigma} \\ + \sum_i \Delta(-ic_{i\uparrow}^\dagger c_{i+x\uparrow} + ic_{i+x\uparrow}^\dagger c_{i\uparrow}^\dagger + c_{i\uparrow}^\dagger c_{i+y\uparrow} + c_{i+y\uparrow}^\dagger c_{i\uparrow}^\dagger) \\ + \sum_i \Delta(ic_{i\downarrow}^\dagger c_{i+x\downarrow} - ic_{i+x\downarrow}^\dagger c_{i\downarrow}^\dagger + c_{i\downarrow}^\dagger c_{i+y\downarrow} + c_{i+y\downarrow}^\dagger c_{i\downarrow}^\dagger) \\ + \sum_i \Delta(ic_{i\uparrow}^\dagger c_{i+z\downarrow} - ic_{i+z\downarrow}^\dagger c_{i\uparrow}^\dagger + ic_{i\downarrow}^\dagger c_{i+z\uparrow} - ic_{i+z\uparrow}^\dagger c_{i\downarrow}^\dagger), \quad (36)$$

where  $\delta = \{x, y, z\}$ . We use  $t = \Delta = 0.5$  and  $\{\mu_1, \mu_2, \mu_3, \mu_4\} = \{4, 3.5, 2.5, 2\}$  in the numerical calculation. Note that besides decaying with  $\mathbf{R}$ , the nonlocal marker  $\mathcal{C}(\mathbf{r} + \mathbf{R}, \mathbf{r})$  shown in Fig. 2(b) also oscillates with  $\mathbf{R}$ . This is a manifestation of the fact that gap closing at the critical point  $\mu_c = 3$  is not located at the  $\Gamma$  point, as explained after Eq. (23).

### C. 3D class AII

The 3D class AII is relevant to prototype TIs such as  $\text{Bi}_2\text{Se}_3$  and  $\text{Bi}_2\text{Te}_3$ . To draw relevance to real materials, we will use the model for the low-energy sector described by the Dirac matrices [41,42]

$$\Gamma_{1\sim 5} = \{\sigma^x \otimes \tau^x, \sigma^y \otimes \tau^x, \sigma^z \otimes \tau^x, I_\sigma \otimes \tau^y, I_\sigma \otimes \tau^z\}. \quad (37)$$

The spinor is  $\psi_{\mathbf{k}} = (c_{\mathbf{k}s\uparrow}, c_{\mathbf{k}p\uparrow}, c_{\mathbf{k}s\downarrow}, c_{\mathbf{k}p\downarrow})^T$ , where  $s$  and  $p$  stand for the  $P1_{\pm}^+$  and  $P2_{\pm}^-$  orbitals in real materials. The low-energy Hamiltonian given by the lowest-order term in the  $\mathbf{k} \cdot \mathbf{p}$  theory,

$$\hat{H} = (M + M_1 k_z^2 + M_2 k_x^2 + M_2 k_y^2) \Gamma_5 + B_0 \Gamma_4 k_z \\ + A_0 (\Gamma_1 k_y - \Gamma_2 k_x), \quad (38)$$

can be regularized on a cubic lattice, yielding [43]

$$H = - \sum_{i\sigma} \mu c_{i\sigma}^\dagger c_{i\sigma} + \sum_{i\sigma} \tilde{M} \{c_{i\sigma}^\dagger c_{i\sigma} - c_{i\sigma}^\dagger c_{i\sigma}\} \\ + \sum_{i\parallel} t_{\parallel} \{c_{i\parallel\uparrow}^\dagger c_{i+a\bar{1}\downarrow} - c_{i+a\bar{1}\uparrow}^\dagger c_{i\bar{1}\downarrow} \\ - ic_{i\parallel\uparrow}^\dagger c_{i+b\bar{1}\downarrow} + ic_{i+b\bar{1}\uparrow}^\dagger c_{i\bar{1}\downarrow} + \text{H.c.}\} \\ + \sum_{i\sigma} t_{\perp} \{-c_{i\sigma}^\dagger c_{i+c\sigma} + c_{i+c\sigma}^\dagger c_{i\sigma} + \text{H.c.}\} \\ - \sum_{i\sigma} M_1 \{c_{i\sigma}^\dagger c_{i+c\sigma} - c_{i\sigma}^\dagger c_{i+c\sigma} + \text{H.c.}\} \\ - \sum_{i\delta\sigma} M_2 \{c_{i\sigma}^\dagger c_{i+\delta\sigma} - c_{i\sigma}^\dagger c_{i+\delta\sigma} + \text{H.c.}\}, \quad (39)$$

where  $\tilde{M} = M + 2M_1 + 4M_2$ ,  $t_{\parallel} = A_0/2$ ,  $t_{\perp} = B_0/2$ ,  $I = \{s, p\}$ , and  $\bar{I} = \{p, s\}$  are the orbital indices,  $\delta = \{a, b, c\}$  denotes the lattice constants, and  $\sigma = \{\uparrow, \downarrow\}$  is the spin index. From Eq. (38), it is clear that the Dirac matrix that has not been used is  $W = \Gamma_3$ , and the normalization factor is  $N_D = -8\pi i$ . In the numerical calculation, we use the parameters  $t_{\parallel} = t_{\perp} = M_1 = M_2 = 1$ , and four values  $\{-2, -1, 1, 2\}$  for the mass term  $M$  to capture the critical behavior near  $M_c = 0$ .

### D. 3D class CII

The minimal model of 3D class CII is a  $8 \times 8$  Dirac model [3], where the seven  $\Gamma$  matrices are given by [4]

$$\Gamma^a = \Gamma_{4 \times 4}^a \otimes \eta_x, \quad \text{for } a = 1 \sim 4, \\ \Gamma^5 = I_{4 \times 4} \otimes \eta_y, \quad \Gamma^6 = I_{4 \times 4} \otimes \eta_z, \\ \Gamma^7 = (-i)^3 \Gamma^1 \Gamma^2 \dots \Gamma^6, \quad (40)$$

where  $\Gamma_{4 \times 4}^a$  are those in Eq. (30). The chiral symmetry is implemented by  $\Gamma^6 = S$ . The Hamiltonian expressed in terms of the other six  $\Gamma$  matrices has a block-off-diagonal form

$$H(\mathbf{k}) = \sum_{i=1,2,3,4,5,7} d_i \Gamma^i = \begin{pmatrix} & & D_{11} & D_{12} \\ & & D_{21} & D_{22} \\ D_{11}^* & D_{12} & & \\ D_{21} & D_{22}^* & & \end{pmatrix}, \\ D_{11} = \begin{pmatrix} h & \\ & h \end{pmatrix} = -D_{22}^*, \quad D_{12} = \begin{pmatrix} g & f \\ f^* & -g^* \end{pmatrix} = D_{21}^\dagger. \quad (41)$$

Within linear Dirac model, we consider

$$\begin{aligned} f &= d_1 - id_2 = Ak_x - iAk_y, & g &= d_3 + id_7 = d_3 = Ak_z, \\ h &= d_4 - id_5 = d_4 = M. \end{aligned} \quad (42)$$

The Dirac matrices that are omitted in the Hamiltonian are  $\{\Gamma^5, \Gamma^6, \Gamma^7\}$ , so we choose  $W = \Gamma^5\Gamma^6\Gamma^7$ , and the normalization factor is  $N_D = -4\pi i/c$ . Since this symmetry class is less explored in the literature, and given that complexity involved in this  $8 \times 8$  model, the examination of the lattice model is left for future investigations.

### E. 3D class CI

For 3D class CI, we resort to the  $8 \times 8$  Hamiltonian expanded by 4 out of the 7 Dirac matrices [3],

$$\begin{aligned} H &= \sum_{i=1}^4 d_i \Gamma_i = \begin{pmatrix} D & \\ & D^\dagger \end{pmatrix}, \\ D &= \begin{pmatrix} D_{21} & D_{12} \end{pmatrix} = \begin{pmatrix} & f^* & -g \\ -f^* & g & -f \\ g^* & f & \end{pmatrix}, \end{aligned} \quad (43)$$

with  $f = d_1 - id_2$  and  $g = d_3 + id_4$ . The  $8 \times 8$  TR and PH operators are  $T = I \otimes I \otimes \sigma_x K$  and  $C = I \otimes I \otimes (-i\sigma_y)K$ , which require  $d_1 \sim d_3$  to be odd in momentum, and  $d_4$  to be the mass term that is even in momentum. Note that we do not need to know the explicit form of the unused  $\Gamma_5 \sim \Gamma_7$  matrices to calculate their product  $W = \Gamma_5\Gamma_6\Gamma_7$ , since we know that

$$\Gamma_1\Gamma_2\Gamma_3\Gamma_4\Gamma_5\Gamma_6\Gamma_7 = \Gamma_1\Gamma_2\Gamma_3\Gamma_4W = cI_{8 \times 8}. \quad (44)$$

Because  $\Gamma_1\Gamma_2\Gamma_3\Gamma_4 = \text{diag}(-1, 1)_{8 \times 8}$ , one sees that  $W = \text{diag}(-c, c)_{8 \times 8} = -cS$  is given by the chiral operator, and  $N_D = -4\pi i/c$ . The exploration of the lattice model corresponding to this  $8 \times 8$  Hamiltonian will be left for further investigations.

## IV. TOPOLOGICAL MARKERS IN TWO DIMENSIONS

For 2D TIs and TSCs, the topological operator reads

$$\hat{C}_{2D} = N_D W [Q\hat{x}P\hat{y}Q - P\hat{x}Q\hat{y}P]. \quad (45)$$

We find that there are only two kinds of topological markers in 2D: For classes A, C, and D that break TR symmetry, the topological marker is the Chern marker [7] described by  $W \propto I$ . On the other hand, the TR-symmetric classes AII and DIII are described by the spin Chern number, yielding a spin Chern marker  $W \propto \sigma_z$  that counts the difference between the spin up and down channels. The numerical calculation using  $20 \times 20$  lattices for all the 5 nontrivial symmetry classes is presented in Fig. 3, as detailed below.

### A. 2D class A

The minimal model of 2D class A is expanded by all three components of Pauli matrices  $H = \sum_{i=1}^3 d_i \sigma_i$ , and the model

regularized on the whole BZ,

$$\begin{aligned} d_1 &= A \sin k_x, & d_2 &= A \sin k_y, \\ d_3 &= M + 4B - 2B \cos k_x - 2B \cos k_y, \end{aligned} \quad (46)$$

gives the Chern insulator, whose lattice model has been given previously [26,43]. Since all Pauli matrices are used, we have  $W = I$ , and the normalization factor is  $N_D = 2\pi i$ . The projection to lattice sites  $|\mathbf{r}\rangle$  is equivalent to the original Chern marker that have been intensively studied [7], and the off-diagonal elements has been called nonlocal Chern markers [26]. Nevertheless, for the sake of completeness of the presentation, we perform simulations using the parameters  $t = A/2 = 1, t' = B = 1, \{M_1, M_2, M_3, M_4\} = \{-2, -0.8, 0.8, 2\}$ .

### B. 2D class D

A concrete system that realizes the 2D class D is the spinless chiral  $p$ -wave SC [3], described by the lattice Hamiltonian

$$\begin{aligned} H &= \sum_{i\delta} t(c_i^\dagger c_{i+\delta} + c_{i+\delta}^\dagger c_i) - \mu \sum_i c_i^\dagger c_i \\ &+ \sum_i \Delta(-ic_i c_{i+x} + ic_{i+x}^\dagger c_i^\dagger + c_i c_{i+y} + c_{i+y}^\dagger c_i^\dagger), \end{aligned} \quad (47)$$

where  $\delta = \{x, y\}$ , and  $c_i$  is the spinless fermion operator at site  $i$ . All three components of Pauli matrices are used, so we also use  $W = I$  and  $N_D = 2\pi i$ . The parameters examined are  $t = -1, \Delta = 0.5, \{\mu_1, \mu_2, \mu_3, \mu_4\} = \{-3, -3.7, -4.3, -5\}$ .

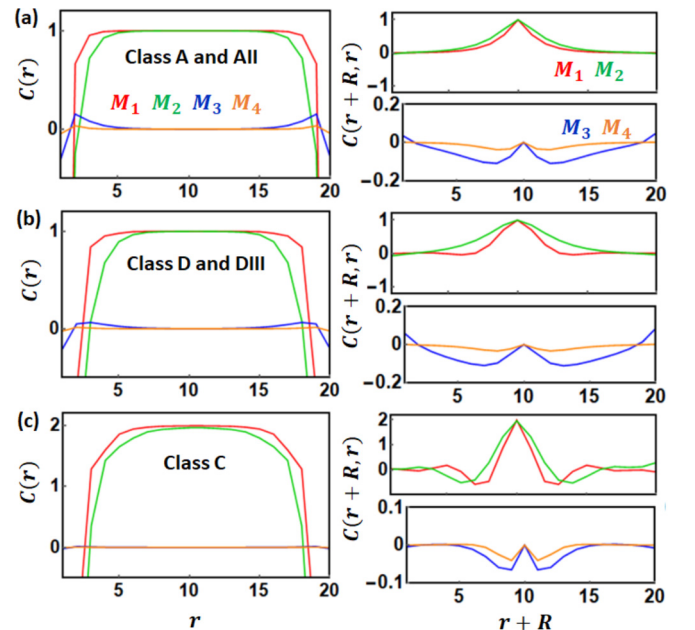


FIG. 3. Local (left column) and nonlocal (right column) topological markers for prototype square lattice models in the five topologically nontrivial symmetry classes in 2D, including (a) the Chern insulator in class A and the BHZ model in class AII that have identical results, (b) the chiral  $p$ -wave SC in class D and helical  $p$ -wave SC in class DIII that have identical results, and (c) a quadratic band crossing model in class C.

### C. 2D class C

The minimal model of the 2D class C is a  $2 \times 2$  Dirac model [33], where the off-diagonal pairing term around the HSP can be expanded by  $d_1 - id_2 = k_+^{n_+} k_-^{n_-}$ , with  $k_{\pm} = k_x \pm ik_y$ . We consider a spinless model of particle-hole basis  $\eta_{\mathbf{k}}^{\dagger} = (c_{\mathbf{k}}^{\dagger}, c_{-\mathbf{k}})$ , where the PH operator  $C = \sigma_y K$  requires all  $d_i(\mathbf{k})$  to be even in momentum; i.e., the model has even-order band crossing at TPTs. For concreteness, we choose to examine the model with the power  $n_+ = 0$ ,  $n_- = 2$ , which may be regularized on a lattice to give the following pairing term,

$$\Delta_{\mathbf{k}} = \Delta(2 \cos k_x - 2 \cos k_y - 2i \sin k_x \sin k_y). \quad (48)$$

This leads us to consider the lattice model that contains both nearest- and next-nearest-neighbor pairings of the same amplitude but a phase difference

$$\begin{aligned} H = & \sum_{i\delta} t(c_i^{\dagger} c_{i+\delta} + c_{i+\delta}^{\dagger} c_i) - \mu \sum_i c_i^{\dagger} c_i \\ & + \Delta \sum_{i, \sigma=\pm} (c_i c_{i+\sigma x} + c_{i+\sigma x}^{\dagger} c_i^{\dagger} - c_i c_{i+\sigma y} - c_{i+\sigma y}^{\dagger} c_i^{\dagger}) \\ & + \frac{\Delta}{2} \sum_i \{-ic_i c_{i+x+y} + ic_i c_{i+x-y} + ic_i c_{i-x+y} - ic_i c_{i-x-y} \\ & + ic_{i+x+y}^{\dagger} c_i^{\dagger} - ic_{i+x-y}^{\dagger} c_i^{\dagger} - ic_{i-x+y}^{\dagger} c_i^{\dagger} + ic_{i-x-y}^{\dagger} c_i^{\dagger}\}. \quad (49) \end{aligned}$$

Since the model already uses all the Dirac matrices, one has  $W = I$  and  $N_D = 2\pi i$ . We use the parameters  $t = 1$ ,  $\Delta = 0.5$ , and  $\{\mu_1, \mu_2, \mu_3, \mu_4\} = \{2, 3, 4.3, 5\}$ . Note that deep inside the bulk and in the topologically nontrivial phase, we obtain  $\mathcal{C}(\mathbf{r}) \approx 2$ , consistent with that expected from the quadratic band crossing [33].

### D. 2D class AII

For 2D class AII that has TR symmetry, we consider the prototype BHZ model with spinful  $s$  and  $p$  orbitals  $\psi = (s\uparrow, p\uparrow, s\downarrow, p\downarrow)^T$ , which uses the Dirac matrices of this model already given in Eq. (34). Interestingly, the unused Dirac matrices combined to give the spin operator  $W = \Gamma_3 \Gamma_4 = iI \otimes \sigma^z$ , and the normalization factor is found to be  $N_D = \pi$ . The diagonal and off-diagonal elements of this topological operator have been called local and nonlocal spin Chern markers previously, whose validity applied to the BHZ model has been elaborated explicitly. The numerical result is exactly the same as the Chern insulator in Sec. IV A if the same parameters are used, as expected since the BHZ model is equivalently two copies of Chern insulators, one for each spin species.

### E. 2D class DIII

The lattice model of 2D class DIII can be obtained from that of the 3D class DIII presented in Sec. III B via a dimensional reduction, which turns off all the  $\sin k_z$  and  $\cos k_z$  terms in the momentum-space Hamiltonian in Eq. (35), and equivalently all the terms that contain  $c_{i+z\sigma}$  or  $c_{i+z\sigma}^{\dagger}$  in the lattice Hamiltonian in Eq. (36). Since we arrange our spinor by  $\eta_{\mathbf{k}}^{\dagger} = (c_{\mathbf{k}\uparrow}^{\dagger}, c_{-\mathbf{k}\uparrow}, c_{\mathbf{k}\downarrow}^{\dagger}, c_{-\mathbf{k}\downarrow})$ , this results in a Hamiltonian that is block-diagonal, where each block corresponds to a

chiral  $p$ -wave SC addressed in Sec. IV B for one spin species, and therefore describes a helical  $p$ -wave SC.

The 3D class DIII model in Sec. III B already omits the  $\Gamma^5$  component, and the dimensional reduction to 2D turns off the  $\Gamma^4$  matrix, so the unused  $\Gamma$  matrices multiplied together  $W = \Gamma^3 \Gamma^5 = iI \otimes \sigma^z$  give the spin polarization operator, indicating that the topological operator is precisely the spin Chern operator discussed in Sec. IV D with a normalization factor  $N_D = \pi$ . Physically, this means that the topological invariant is given by the difference between the Chern number of the spin up chiral  $p$ -wave SC and that of the spin down component. As a result, the spin Chern marker of the helical  $p$ -wave SC is identical to the Chern marker of the chiral  $p$ -wave SC given in Sec. IV B at the same parameters.

## V. TOPOLOGICAL MARKERS IN ONE DIMENSION

The topological operator in 1D takes the form

$$\hat{\mathcal{C}}_{1D} = N_D W [Q \hat{x} P + P \hat{x} Q]. \quad (50)$$

Interestingly, for all the symmetry classes in 1D that preserve chiral symmetry (AIII, BDI, CII, DIII), the product of unused Dirac matrices is always proportional to the chiral operator  $W \propto S$ , whereas the class D that does not preserve chiral symmetry has a different interpretation of  $W$ . The numerical results for these 5 classes are given in Fig. 4 and are described in detail below.

### A. 1D class BDI

For 1D class BDI, we use the prototype spinless Su-Schrieffer-Heeger (SSH) model as an example, which is described by the lattice Hamiltonian [44]

$$\mathcal{H}_0 = \sum_i (t + \delta t) c_{Ai}^{\dagger} c_{Bi} + (t - \delta t) c_{Ai+1}^{\dagger} c_{Bi} + \text{H.c.}, \quad (51)$$

where  $c_{Ai}$  and  $c_{Bi}$  are the fermion annihilation operators on sublattice  $A$  and  $B$  in the unit cell  $i$ , respectively, and  $t \pm \delta t$  are the alternating hopping amplitudes. The  $2 \times 2$  Hamiltonian expressed in momentum space with the basis  $(c_{Ak}, c_{Bk})$  is expanded by  $\sigma_x$  and  $\sigma_y$ , so the only Pauli matrix that has not been used is the chiral operator  $W = S = \sigma_z$ , and the normalization factor is unity  $N_D = 1$ . Note that as discussed after Eq. (8), to realize the position operator  $\hat{x}$  as a diagonal matrix, the  $A$  and  $B$  sublattices within the same unit cell located at  $i$  are assigned with the same position  $x_i$ , even though they are frequently drawn as a certain distance apart. We choose parameters  $t = 1$ ,  $\{\delta t_1, \delta t_2, \delta t_3, \delta t_4\} = \{-0.5, -0.2, 0.2, 0.5\}$  and 20 lattice sites in the numerical simulation, and the gap-closing momentum is located at  $k_0 = \pi$  for the critical point  $\delta t_c = 0$ , yielding an oscillating and decaying nonlocal marker  $\mathcal{C}(r+R, r)$  as shown in Fig. 4(a). Some other 1D models investigated below also show an oscillating  $\mathcal{C}(r+R, r)$  for the same reason.

### B. 1D class AIII

The low-energy linear Dirac model [33] for 1D class AIII can be expanded by  $H(\mathbf{k}) = Ak_x \sigma_x + M \sigma_z$ , with the unused Pauli matrix being the chiral symmetry operator  $W = S = \sigma_y$  and the normalization factor  $N_D = 1$ . The regularization in

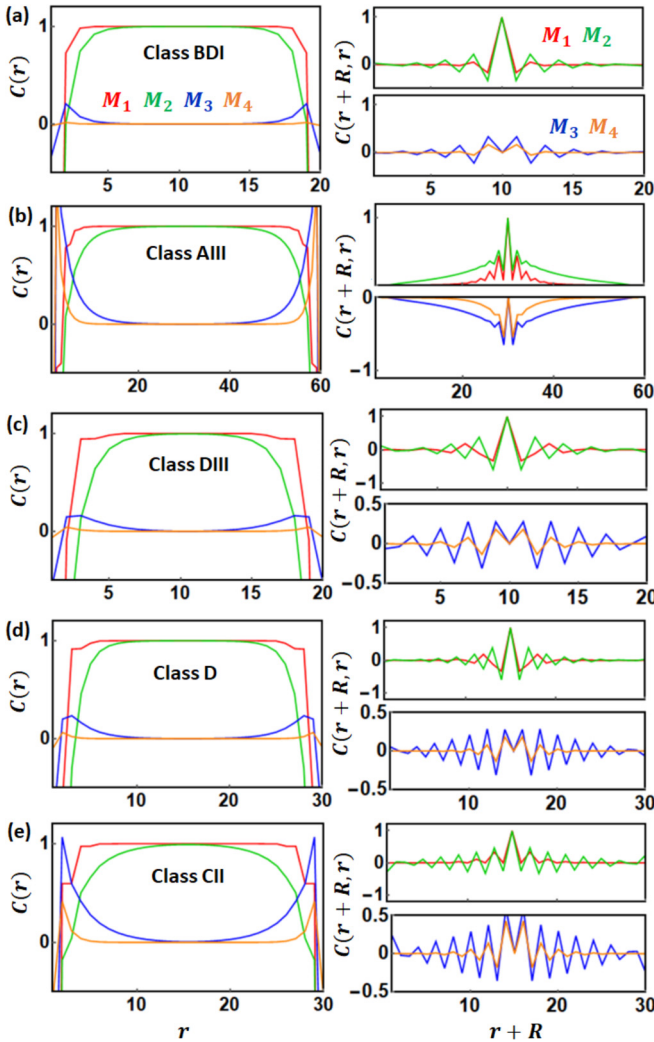


FIG. 4. Local (left column) and nonlocal (right column) topological markers for the lattice models in the five topologically nontrivial symmetry classes in 1D, including (a) the SSH model in class BDI, (b) a regularized lattice model in class AIII, (c) a class DIII model obtained from dimensional reduction, (d) the Kitaev  $p$ -wave SC chain in class D, and (e) a regularized lattice model in class CII.

Eqs. (31) and (32) leads to a lattice model

$$\begin{aligned}
 H = & \sum_i (M - 2t')(c_{i1}^\dagger c_{i1} - c_{i2}^\dagger c_{i2}) \\
 & + \sum_i t'(c_{i1}^\dagger c_{i+x1} + c_{i+x1}^\dagger c_{i1} + c_{i2}^\dagger c_{i+x2} + c_{i+x2}^\dagger c_{i2}) \\
 & + \sum_i t(-ic_{i1}^\dagger c_{i+x2} + ic_{i+x2}^\dagger c_{i1} - ic_{i2}^\dagger c_{i+x1} + ic_{i+x1}^\dagger c_{i2}).
 \end{aligned} \tag{52}$$

We have used  $t = 1$ ,  $t' = 0.4$ ,  $\{M_1, M_2, M_3, M_4\} = \{0.6, 0.2, -0.2, -0.6\}$ , and 60 lattice sites in the numerical simulation.

### C. 1D class DIII

We construct a lattice model of 1D class DIII by performing dimensional reduction twice on the 3D class DIII model in Sec. III B, which is done by turning off all the  $\{\sin k_y, \sin k_z, \cos k_y, \cos k_z\}$  terms in Eq. (35), and analogously turning off all the  $\{c_{i+y\sigma}, c_{i+y\sigma}^\dagger, c_{i+z\sigma}, c_{i+z\sigma}^\dagger\}$  terms in Eq. (36). The resulting Hamiltonian omits  $\{\Gamma^2, \Gamma^4, \Gamma^5\}$  matrices defined in Eq. (34), so  $W = \Gamma^2 \Gamma^4 \Gamma^5 = S$  is given by the chiral operator, and the normalization factor is  $N_D = i/2$ . We use the parameters  $t = 1$ ,  $\Delta = 0.5$ ,  $\{\mu_1, \mu_2, \mu_3, \mu_4\} = \{1, 1.8, 2.2, 3\}$  and 20 lattice sites in the numerical calculation.

### D. 1D class D

For 1D class D, we examine the spinless Kitaev  $p$ -wave SC chain described by [45]

$$\begin{aligned}
 H = & \sum_i t(c_i^\dagger c_{i+1} + c_{i+1}^\dagger c_i) - \mu \sum_i c_i^\dagger c_i \\
 & + \sum_i \Delta(c_i c_{i+1} + c_{i+1}^\dagger c_i^\dagger),
 \end{aligned} \tag{53}$$

where  $c_i$  is the spinless fermion annihilation operator at site  $i$ . The Hamiltonian in momentum space in the basis of  $(c_k, c_{-k}^\dagger)^T$  is spanned by  $\sigma_z$  and  $\sigma_y$ , so the only Pauli matrix that has not been used is  $W = \sigma_x$ , and  $N_D = 1$ . A 30-site lattice with the parameters  $t = 1$ ,  $\Delta = 0.5$ ,  $\{\mu_1, \mu_2, \mu_3, \mu_4\} = \{1, 1.8, 2.2, 3\}$  is used in the numerical simulation.

### E. 1D class CII

For 1D class CII, we adopt the  $\Gamma$  matrices [46]

$$\Gamma^a = \{\sigma_x \otimes \tau_z, \sigma_y \otimes \tau_z, I \otimes \sigma_x, I \otimes \tau_y, \sigma_z \otimes \tau_z\}, \tag{54}$$

and the TR and PH operators are interpreted by  $T = \sigma_y \otimes IK$  and  $C = I \otimes \tau_y K$ . The minimal model in momentum space is  $H = d_2 \Gamma^2 + d_3 \Gamma^3 = Ak\Gamma^2 + M\Gamma^3$ , and we denote the spinor by  $\psi_k^\dagger = (c_{1k}^\dagger, c_{2k}^\dagger, c_{3k}^\dagger, c_{4k}^\dagger)$  where the four degrees of freedom are enumerated by  $1 \sim 4$ . The regularization on a lattice gives

$$\begin{aligned}
 H = & \sum_i t\{-c_{i1}^\dagger c_{i+x2} + c_{i2}^\dagger c_{i+x1} + c_{i3}^\dagger c_{i+x4} - c_{i4}^\dagger c_{i+x3}\} \\
 & + \sum_i (-t')\{c_{i1}^\dagger c_{i+x3} + c_{i3}^\dagger c_{i+x1} + c_{i2}^\dagger c_{i+x4} + c_{i4}^\dagger c_{i+x2}\} \\
 & + \sum_i (M + 2t')\{c_{i1}^\dagger c_{i3} + c_{i2}^\dagger c_{i4}\} + \text{H.c.}
 \end{aligned} \tag{55}$$

The unused Dirac matrices multiplied together are proportional to the chiral operator  $W = \Gamma^1 \Gamma^4 \Gamma^5 = -iS$ , and the normalization factor is  $N_D = i/2$ . We use the parameters  $t = 1$ ,  $t' = 0.5$ ,  $\{M_1, M_2, M_3, M_4\} = \{-1, -1.8, -2.2, -3\}$  and a 30-site lattice in the simulation.

## VI. CONCLUSIONS

In summary, we show that topological marker can be constructed in a unified manner for TIs and TSCs in any dimension and symmetry class. The central object in our formalism is the topological operator in Eq. (15) derived

from the universal topological invariant in momentum space, which takes the form of alternating projectors to the lattice eigenstates and the position operators, multiplied by the Dirac matrices that are omitted in the Hamiltonian. The  $r$ th diagonal element of the topological operator gives the local topological marker that recovers the topological invariant for lattice sites deep inside the bulk. In addition, the  $(\mathbf{r} + \mathbf{R}, \mathbf{r})$ th off-diagonal element yields a nonlocal topological marker that decays with  $\mathbf{R}$ , whose decay length diverges at TPT and may be interpreted as a Wannier state correlation function, thereby serving as a faithful correlator to identify TPTs in real space. The topological operator is constructed explicitly for each of the 15 topologically nontrivial symmetry classes in 1D to 3D. For 13 out of these 15 cases, we perform numerical calculation on concrete lattice models to demonstrate the validity of our topological marker, which cover a great number of prototype TIs and TSCs including the SSH model, Majorana chain, Chern insulator, BHZ model, chiral and helical  $p$ -wave SCs, 3D TR invariant TIs, lattice model of  $^3\text{He}$  B-phase, among many others, suggesting the ubiquity of our formalism.

Our results point to many open questions that remain to be clarified. First, it is known that the deviation of the Chern marker at the boundary sites of the 2D lattice, which occurs even if the periodic boundary condition is imposed, comes from the fact that the position operators  $\hat{i}$  in Eq. (15) do not respect the translational invariance, and may be cured by exponentiating the position operators [8–10]. Whether such an exponentiating trick can be generally applied to topological markers in any dimension and symmetry class, and whether it has some noncommutative interpretation on the topological order in general, remains to be investigated. Second, a major category of topological materials that we did not

address are the topological semimetals in  $D$  dimensions, such as graphene in 2D, in which the momentum-space topological invariant is the wrapping number in Eq. (1) but integrated over a  $(D - 1)$ -dimensional surface enclosing a nodal point. Because the momentum integration is one dimension lower, it is unclear to us at present whether the projector algebra in Sec. II A still applies, or how it may be modified to construct a topological marker for semimetals. Third, concerning the experimental measurement of the topological marker, it has been pointed out that the Chern marker in 2D TR-breaking systems can be measured by circular dichroism [26], and the spin-Chern marker in 2D TR-symmetric systems can be detected by spin-resolved circular dichroism [27]; both are due to the linear response of valence electrons to polarized electric field. However, because TIs and TSCs in other dimensions do not respond linearly to the electric field [47], it remains to be investigated whether higher-order responses can help to extract the topological marker in other dimensions, or whether one has to resort to some other kind of experimental protocol. Finally, we emphasize that our formalism is based on the momentum-space topological invariant in Eq. (1) applicable only to Dirac Hamiltonians, and consequently the resulting universal topological marker is also applicable only to lattice Dirac models, which nevertheless covers a great variety of theoretical models. An obvious question is then whether our marker will still remain quantized for systems that are beyond the paradigm of Dirac models, such as 2D class AII systems with spin-orbit coupling [48], of which only concrete calculations can tell. All these open questions, together with the applications of the universal topological marker on issues such as real-space inhomogeneity, interfaces, and interacting or periodically driven systems, are intriguing subjects that await to be explored.

- 
- [1] M. Z. Hasan and C. L. Kane, *Rev. Mod. Phys.* **82**, 3045 (2010).
- [2] X.-L. Qi and S.-C. Zhang, *Rev. Mod. Phys.* **83**, 1057 (2011).
- [3] A. P. Schnyder, S. Ryu, A. Furusaki, and A. W. W. Ludwig, *Phys. Rev. B* **78**, 195125 (2008).
- [4] S. Ryu, A. P. Schnyder, A. Furusaki, and A. W. W. Ludwig, *New J. Phys.* **12**, 065010 (2010).
- [5] A. Kitaev, *AIP Conf. Proc.* **1134**, 22 (2009).
- [6] C.-K. Chiu, J. C. Y. Teo, A. P. Schnyder, and S. Ryu, *Rev. Mod. Phys.* **88**, 035005 (2016).
- [7] R. Bianco and R. Resta, *Phys. Rev. B* **84**, 241106(R) (2011).
- [8] E. Prodan, T. L. Hughes, and B. A. Bernevig, *Phys. Rev. Lett.* **105**, 115501 (2010).
- [9] E. Prodan, *New J. Phys.* **12**, 065003 (2010).
- [10] E. Prodan, *J. Phys. A: Math. Theor.* **44**, 113001 (2011).
- [11] T. A. Loring and M. B. Hastings, *Europhys. Lett.* **92**, 67004 (2010).
- [12] R. Bianco and R. Resta, *Phys. Rev. Lett.* **110**, 087202 (2013).
- [13] I. Mondragon-Shem, T. L. Hughes, J. Song, and E. Prodan, *Phys. Rev. Lett.* **113**, 046802 (2014).
- [14] A. Marrazzo and R. Resta, *Phys. Rev. B* **95**, 121114(R) (2017).
- [15] F. Cardano, A. D’Errico, A. Dauphin, M. Maffei, B. Piccirillo, C. de Lisio, G. De Filippis, V. Cataudella, E. Santamato, L. Marrucci, M. Lewenstein, and P. Massignan, *Nat. Commun.* **8**, 15516 (2017).
- [16] E. J. Meier, F. A. An, A. Dauphin, M. Maffei, P. Massignan, T. L. Hughes, and B. Gadway, *Science* **362**, 929 (2018).
- [17] H. Huang and F. Liu, *Phys. Rev. B* **98**, 125130 (2018).
- [18] H. Huang and F. Liu, *Phys. Rev. Lett.* **121**, 126401 (2018).
- [19] B. Focassio, G. R. Schleder, F. Crasto de Lima, C. Lewenkopf, and A. Fazzio, *Phys. Rev. B* **104**, 214206 (2021).
- [20] J. Sykes and R. Barnett, *Phys. Rev. B* **103**, 155134 (2021).
- [21] L. Jezequel, C. Tauber, and P. Delplace, *J. Math. Phys.* **63**, 121901 (2022).
- [22] C. Wang, T. Cheng, Z. Liu, F. Liu, and H. Huang, *Phys. Rev. Lett.* **128**, 056401 (2022).
- [23] J. D. Hannukainen, M. F. Martinez, J. H. Bardarson, and T. K. Kvornring, *Phys. Rev. Lett.* **129**, 277601 (2022).
- [24] X. Liu, F. Harper, and R. Roy, *Phys. Rev. B* **98**, 165116 (2018).
- [25] C. Tauber, *Phys. Rev. B* **97**, 195312 (2018).
- [26] P. Mognini, B. Lapiere, R. Chitra, and W. Chen, *arXiv:2207.00016*.
- [27] W. Chen, *arXiv:2207.02973*.
- [28] G. von Gersdorff, S. Panahiyan, and W. Chen, *Phys. Rev. B* **103**, 245146 (2021).
- [29] W. Chen, *J. Phys.: Condens. Matter* **28**, 055601 (2016).

- [30] W. Chen, M. Sigrist, and A. P. Schnyder, *J. Phys.: Condens. Matter* **28**, 365501 (2016).
- [31] W. Chen, M. Legner, A. Rüegg, and M. Sigrist, *Phys. Rev. B* **95**, 075116 (2017).
- [32] W. Chen and M. Sigrist, *Advanced Topological Insulators* (Wiley-Scrivener, Hoboken, NJ, 2019), Chap. 7.
- [33] W. Chen and A. P. Schnyder, *New J. Phys.* **21**, 073003 (2019).
- [34] J. P. Provost and G. Vallee, *Commun. Math. Phys.* **76**, 289 (1980).
- [35] G. von Gersdorff and W. Chen, *Phys. Rev. B* **104**, 195133 (2021).
- [36] S. Panahiyan, W. Chen, and S. Fritzsche, *Phys. Rev. B* **102**, 134111 (2020).
- [37] R. Balian and N. R. Werthamer, *Phys. Rev.* **131**, 1553 (1963).
- [38] G. E. Volovik, *The Universe in a Helium Droplet* (Oxford University Press, New York, 2009).
- [39] B. A. Bernevig, T. L. Hughes, and S.-C. Zhang, *Science* **314**, 1757 (2006).
- [40] M. König, S. Wiedmann, C. Brüne, A. Roth, H. Buhmann, L. W. Molenkamp, X.-L. Qi, and S.-C. Zhang, *Science* **318**, 766 (2007).
- [41] H. Zhang, C.-X. Liu, X.-L. Qi, X. Dai, Z. Fang, and S.-C. Zhang, *Nat. Phys.* **5**, 438 (2009).
- [42] C.-X. Liu, X.-L. Qi, H. J. Zhang, X. Dai, Z. Fang, and S.-C. Zhang, *Phys. Rev. B* **82**, 045122 (2010).
- [43] W. Chen, *Phys. Rev. B* **101**, 195120 (2020).
- [44] W. P. Su, J. R. Schrieffer, and A. J. Heeger, *Phys. Rev. Lett.* **42**, 1698 (1979).
- [45] A. Y. Kitaev, *Phys. Usp.* **44**, 131 (2001).
- [46] Y. X. Zhao and Z. D. Wang, *Phys. Rev. B* **90**, 115158 (2014).
- [47] B. A. Bernevig and T. L. Hughes, *Topological Insulators and Topological Superconductors* (Princeton University Press, Princeton, NJ, 2013).
- [48] C. L. Kane and E. J. Mele, *Phys. Rev. Lett.* **95**, 226801 (2005).